

JPL NO 9950 - 1050

MSAT-X Report No. 105

956528

Propagation Considerations in Land Mobile Satellite Transmission

by

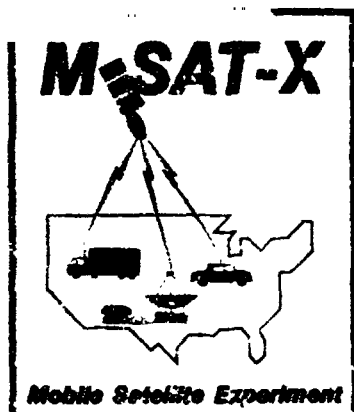
Wolfhard J. Vogel

University of Texas at Austin

and

Ernest K. Smith

Jet Propulsion Laboratory



An MSAT-X Report by
The University of Texas at Austin and JPL

24 January, 1985



National Aeronautics and
Space Administration

Jet Propulsion Laboratory
California Institute of Technology
Pasadena, California

(D)SA-Ca-175733) PROPAGATION CONSIDERATIONS
IN LAND MOBILE SATELLITE TRANSMISSION (Jet
Propulsion Lab.) 20 DEC 1983/MF AG1

825-25684

CSCI 17B

Unclassified
G3/32 211 6

MSAT-X Report No. 105

PROPAGATION CONSIDERATIONS IN
LAND MOBILE SATELLITE TRANSMISSION

by

Wolfhard J. Vogel
University of Texas at Austin

and

Ernest K. Smith, JPL

24 January, 1985

PREFACE

The work described in this report was jointly supported by the MSAT-X program and the NASA Propagation Studies and Measurements program. Wolf Vogel and I wrote this article during a visit I made to Texas in November, 1984 just prior to the successful dedicated balloon launch of November 12 and 13 (Texas to Alabama).

We divided up the writing. I wrote Sections 1, 2 and 5; and Wolf Vogel wrote Sections 3, 4 and 6. Firouz Naderi, Task Manager for MSAT-X, substantially rewrote the Introduction (Section 1) in the editorial review process. By rights, he should be a co-author; but making him one would be counter to the ethics of manuscript review.


Ernest K. Smith
Propagation Coordinator

January 24, 1985

Abstract

It now appears likely that the Land Mobile Satellite Services (LMSS) will be authorized by the FCC for operation in the 800 to 900 MHz ("UHF") and possibly near 1500 MHz ("L-band"). Propagation problems are clearly an important factor in the effectiveness of this service, but useful measurements are few, and have produced contradictory interpretations. This report provides a first-order overview of existing measurements with particular attention to the first two NASA balloon-to-mobile vehicle propagation experiments. The report also provides some physical insight into the interpretation of propagation effects in LMSS transmissions.

. INTRODUCTION

The land mobile satellite service (LMSS) is under active consideration by the FCC for U.S. frequency allocation at 800 to 900 MHz ("UHF") and possibly at 1500 to 1700 MHz ("L-band"). While the outcome of FCC notice of proposed rulemaking is still not clear, it seems likely that the LMSS in some form will materialize.

A Mobile Satellite System (MSS) is a satellite-based communications network that provides voice and data communications to mobile users throughout a vast geographical area. The operation is similar to a terrestrial-based land mobile communications system in which vehicles within lines-of-sight of ground-based transmitting towers can communicate with each other. The difference is that the satellite system, with its "relay tower" placed at a height of 22,000 miles (the parking orbit for geostationary satellites), can extend the effective line of sight substantially and provide uninterrupted blanket coverage over an extremely large area such as the North American continent.

Propagation considerations turn out to be a major factor in the design and viability of land mobile satellite systems. The fundamental problem of communicating with mobile users via satellite links stems from the small size and limited performance inherent in low cost vehicle terminals, in general and in vehicle antennas in particular. In LMSS, where the ground terminals are either portable or mobile, multipath fading and shadowing make the channel much more hostile than either broadcast or fixed satellite services.

In recent years, NASA has undertaken a number of system studies to determine what the driving technologies and critical design issues will be on the MSS satellites of the future. These studies by JPL (Naderi, et. al., 1982) and TRW (Horstein, 1983) all point out that the future high capacity MSS will be severely constrained by shortages in spectrum, orbital slot and spacecraft e.i.r.p. Propagation impairments in the mobile channel, particularly multipath fading and shadowing by man-made and natural obstructions exacerbate the spacecraft e.i.r.p. shortage. The problem is further complicated since there is little relevant experimental data which adequately characterizes the fading channel at the frequencies of interest to LMSS.

1.1 Mobile Satellite Experiment (MSAT-X)

In order to better characterize the LMSS channel and to develop and validate advanced ground segment technologies, including vehicle antennas, NASA intends to enter into a barter type agreement with the U.S. commercial entity licensed by FCC to implement the first generation LMSS. Under this agreement, NASA would provide free satellite launch services to the satellite. Subsequently, NASA will use this capacity to validate advanced technologies and to conduct propagation experiments using a variety of vehicle antennas including both omni directional and steerable antennas. (It should be noted that the propagation characteristics of a fading channel are strongly dependent on the type of the vehicle antenna employed). The expected experimental period for MSAT-X is 1988-1990 [For more information on MSAT-X see the MSAT-X paper by Naderi, et. al., October, 1984].

1.2 Past and Present Activities

During the latter phases of the Applications Technology Satellite (ATS) effort, NASA participated in mobile experiments using ATS-6 beacons with Motorola (Hess 1978, 1980) at 860 MHz and the General Electric Company (Anderson, et. al., 1981) at 1550 MHz.

2. Theory

Shown in Figure 1 is an artist's conception of the LMSS problem from the propagation standpoint. As it is customary to include the natural noise background under "propagation," that should have been shown in the figure as well, but it is already rather busy. In Figure 1 the ray r_1 is the direct path from satellite to mobile antenna. With most satellite systems the problem stops after consideration of r_1 , first as it is affected by the ionosphere and then the troposphere. In LMSS it is also necessary to consider the ray (or bundle of rays) r_2 which is reflected specular at the Fresnel zones on the ground in the direction of the satellite. Finally, there are those rays r_3 which represent power scattered into the antenna main beam and side lobes from discontinuities in the terrain which cause the so-called "diffuse" component. In this section the direct ray will be treated first, then the ground reflected ray, then the diffuse ray, and finally the composite of the three rays.

2.1 The direct ray, r_1 passes through the ionosphere where the total electron column (TEC) in the presence of the Earth's magnetic field, will cause a rotation of the plane of polarization (Faraday rotation) and a modest delay in the signal. Occasionally the variability in the electron density will cause scintillation of the signal amplitude, phase, and direction of arrival.

2.1.1 Faraday Rotation is rotation of the polarization axis of a non-circularly polarized wave as it travels through the ionosphere. The electromagnetic wave splits into two orthogonal components (ordinary and extraordinary) as it enters the ionosphere, recombining as it leaves. As the phase velocities for the two components are slightly different, the recombined wave experiences a rotation of its polarization vector in the plane normal to direction of propagation according to:

$$\Omega = \frac{2.36}{2} \int_{f \text{ Hz}} B_L \text{ (Gauss) } N \text{ ds radians} \quad (1)$$

where B_L is the component of the Earth's magnetic field along the ray path, N is the electron density in electrons per meter cubed, and f is the frequency in Hertz. If we take $B_L = -0.4$ gauss at 400 Km for typical propagation paths to geostationary satellites in North America one can crudely approximate (1) by

$$\Omega \approx \frac{0.5 \text{ (TEC)}}{f^2 \text{ GHz}} \text{ degrees} \quad (2)$$

where TEC is in hexels (10^{16} electrons per m^2).

Thus a value of 100 TEC units (10^{18} esu/m²) would result in a Faraday rotation of about 70 degrees at 850 MHz and about 20 degrees at 1.6 GHz. If the transmitting and receiving antennas are co-polar, then the polarization loss would be $20 \log (\cos \Omega)$ dB or 9.3 dB at 850 MHz but only 0.5 dB at 1.6 GHz. The CCIR uses a value of $\Omega = 108^\circ$ at 1 GHz as the maximum Faraday rotation to be expected at 1 GHz. This is in good agreement with the Japanese results from ETS-II shown in Figure 2 for a mid-latitude station to a geostationary satellite (CCIR Rep. 263-5) converted to the frequencies and elevation angles of interest here. The base data is a full year of recordings during a period of solar maximum 1979-80 (Zurich sunspot number around 157) and a period of low sunspot number (Zurich sunspot number around 42). As can be seen at 850 MHz Faraday rotation will cause significant losses to linearly polarized antennas so that circular polarization is indicated. The same does not hold for 1.6 GHz where the worst 1% of the time of the worst year yields a rotation of 42.7 degrees leading to a loss of -2.7 dB between linear antennas.

2.1.2 Ionospheric Scintillation is most severe at low latitudes (about 9° N to 31° S in the Americas) and next at auroral latitudes (above about 59° N latitude for transmission to geostationary orbit in eastern North America). Mid-latitude scintillation will be less of an impairment and has been ignored in most LMSS analyses. A good discussion is given in CCIR Report 263-5 (1982).

2.2 Ground Reflection. The most likely surface for the ground reflected wave (ray r_2) to impinge upon is paving (concrete, asphalt or dirt) inasmuch as the reflection points for elevation angles of 20° to 60° and an assumed antenna height of 2 m are 5.5 m and 1.2 m from the mobile antenna, respectively. If the mobile were a boat or a hiker then the situation would be vastly different. Shown in Figure 3 are curves of the plane Earth reflection coefficients (vertical polarization) for several different situations. For horizontal polarization the reflection coefficient decreases monotonically from unity at 0° elevation angle to the vertical polarization value at zenith. Vertical polarization has a Brewster (or pseudo-Brewster) angle at which point the amplitude of the reflection coefficient approaches zero and the phase angle shifts from near 180° to near 0° . Note also that the magnitude of the vertical reflection coefficient is always less than that for horizontal polarization. As a consequence, a circularly polarized wave will always look somewhat elliptical upon ground reflection, but more significantly it will have its direction of rotation reversed at elevation angles above the Brewster angle (6° to 27°). This latter characteristic is important to mobile antenna design.

The magnitude of the ground-reflected wave is given by

$$E_2 = \rho_s D R_0 E_1 \quad . \quad (3)$$

where: ρ_s is called the terrain roughness factor,

D is the divergence factor (taken as 1),

R_0 is the plane Earth reflection coefficient.

The magnitude of ρ_s is given by Beckmann and Spizzichino (1963) as

$$\rho_s = e^{-\frac{-(\Delta\phi)^2}{2}} \quad (4)$$

$$\text{where } \Delta\phi = \frac{4\pi \Delta h \sin\psi}{\lambda} \quad (5)$$

and Δh is the rms height of irregularities of the surface,

ψ is the elevation angle at the ground reflection point,

and λ is the wavelength.

A plot of this relationship is given in Figure 4. There has been concern that the drop off is too fast. A recent paper by Miller, Brown & Vehg (1984) suggests that equation (4) should be written

$$\rho_s = e^{-\frac{-(\Delta\phi)^2}{2}} I_0 \left[\frac{(\Delta\phi)^2}{2} \right] \quad (6)$$

where I_0 is the modified Bessel function. This has the property of moderating the rapid decrease of ρ_s with $\Delta\phi$ which otherwise occurs (see Figure 4).

2.3 The Diffuse Component. The ray r_3 in Figure 1 represents the biggest unknown in the terrain multipath question. It may represent a composite return from a recently plowed field or an almost specular reflection from the face of a rock formation like the Flatirons near Boulder, Colorado. The current treatment of this "diffuse component" is to assume that it is Rayleigh distributed and has an rms level which is 8 to 14 dB below the direct ray E_1 . Whereas, the ground-reflected component E_2 is, by definition arriving at $-\theta$, where $+\theta$ is the elevation angle of the satellite as seen from the mobile, the assumption is that the diffuse component arrives, to a first approximation, at 0° (i.e., horizontally). The second order approximation would consider it distributed between $-$ and, say, $+10^\circ$ in elevation with a maximum at 0° . A major uncertainty at present is just what this diffuse component for the land mobile case will turn out to be on a statistical basis. The maritime mobile situation is better understood, probably because there are regularities in the ocean situation (waves move in the same direction, and the relationship of wind and wave structure is well understood).

2.4 Combination of the Three Components. The combination of the energy in the three ray paths (r_1 , r_2 , r_3) shown in Figure 1 is usually accomplished as follows. One first assumes that the fading rate of the direct component E_1 (ray path r_1) plus the specular or coherently ground-reflected component E_2 (ray path r_2) is significantly less than the diffuse component E_3 (represented by ray path r_3) and that the amplitude of this combination is probably not much different in level from E_1 . Hence, their vector sum is

$$\begin{array}{c} \rightarrow \quad \rightarrow \quad \rightarrow \\ E'_1 = E_1 + E_2 \approx E_1 \end{array} \quad (7)$$

In practice the reduction of the ground reflected relative to the direct component is assisted by antenna directivity at the mobile. This resultant, which we will call E'_1 is then combined with the diffuse component E_3 (which is taken to be Rayleigh distributed) and this second resultant distribution can then be described in terms of Rician statistics. The Rice distribution (or Rice-Nakagami distribution) describes the combination of a steady signal and a Rayleigh distributed signal in terms of the relative rms power in the two components. Such a distribution is shown in Figure 10.

2.5 Foliage Blockage. Roadside trees may turn out to be the limiting propagation impairment to LMSS. Studies such as that by Hess (1980) have stressed the importance of side of the street and direction of a street relative to the satellite to mobile path, but primarily for the urban situation. It appears that, for a significant fraction of the U.S., roadside trees constitute an important signal blockage factor, occasionally even at zenith angles. On the multilane E-W interstate highways westward moving traffic will be essentially free from foliage blockage but not eastward traffic. Horace Dewey (Go West Young Man) was a hundred years before his time! Similarly, N-S roads should show less blockage for transmission to a satellite at the same longitude than would be expected for E-W roads, but generalizations are dangerous.

Foliage attenuation has received a lot of attention for ground-to-ground paths (see for example CCIR Rep 236-5) and paths diffracting over the tree tops have been successfully employed. Weissberger (1981) has suggested that for cases where one terminal is near a small (less than 400 m deep) grove, the additional loss L can be predicted by the formula

$$L = 0.187 f^{0.284} d^{0.588} \text{ dB} \quad (8)$$

where f is the frequency in MHz, and d is the depth of the grove traversed by the direct ray (r_1 in Fig. 1) in meters. This equation is said to be applicable from 200 to 95,000 MHz. At its Interim Meeting in 1983, CCIR Study Group 5 proposed a simpler form of this relation, namely

$$L = 0.2 f^{0.3} d^{0.6} \text{ dB} \quad (9)$$

The difference between the two formulas is not great but neither is it negligible. For example, at 1 GHz a 10 m path through foliage gives 5.15 dB by formula (8) and 6.32 dB by formula (9). It is also difficult in view of Lambert's law to justify an exponent different from one for the distance term in equations (8) and (9).

2.6

Fading Rate. Consider the rate of fading which could occur between E_1 and any ray E_3 in Figure 5 which depicts a mobile vehicle at A moving towards the satellite with velocity. A stationary obstacle (B) behind the mobile reflects a signal back into the antenna along r_3+ . Two Doppler frequency shifts, in opposite directions are then observed. The direct signal will be shifted upwards by

$$f_{r_1} = + \frac{v}{c} f_T \cos \theta \quad (10)$$

The reflected signal will be shifted downwards by

$$f_{r_3} = - \frac{v}{c} f_T \quad (11)$$

where C is the velocity of light and f_T the transmission frequency. The frequency difference Δf between these two signals is

$$\Delta f = f_{r_1} - f_{r_3} = \frac{v}{c} f_T (\cos \theta + 1) \quad (12)$$

In the limit ($\cos \theta = 1$) this becomes

$$\Delta f = \frac{2vf_T}{c} = \frac{2v}{\lambda} \quad (13)$$

For example, if $f_T = 850$ MHz, $\theta = 30^\circ$ and $v = 100$ km/hr, Δf from (12) is 146.86 Hz and from (13) is 157.41 Hz. These are first order estimates of the maximum expected frequency of fading.

Figure 5 can also be used to derive the standing wave pattern on the road. The null to null distance represents 360° change in phase with distance Δr along the ground, but the phase path is also reduced along by r_3 by $\Delta r \cos \theta$.

$$\begin{aligned} \Delta r + \Delta r \cos \theta &= \lambda \\ \Delta r &= \lambda / (1 + \cos \theta) \end{aligned} \quad (14)$$

In the limit (elevation angle $\theta = 0$) Δr , the null to null distance is equal to $\lambda/2$. This is the argument for taking data every eighth wavelength of traverse along the ground path.

The question of maximum fading frequency due to blockage can be formulated by creating Fresnel zones (loci of $r + n/2$) at the distance of an obstruction, say a telephone pole, in the path of the direct ray. The pieces of the Cornu spiral can then be reconstituted to provide a measure of the dimensions of an obstruction which will produce a significant decrease (or increase) in signal level. The first Fresnel zone radius is $F_1 = \sqrt{\lambda d}$ where d is the distance from the mobile to the obstruction. Let $d = 20$ m and $\lambda = 0.353$ m, then $F_1 = 2.66$ m. If obstructing $0.1 F_1$ is serious then at 100 km/the fade rate N is given by

$$N = \frac{10^5}{3600(2.66)} = 104.4 \text{ Hz}$$

Noise. The noise environment about the satellite (see for example CCIR Rep 720-1) will be the ground in the main beam of its antenna, while sidelobes may pick up the oceans and galactic and solar noise. At 850 MHz the brightness temperature of the land seen at 45° incidence might be 260K, that of water 94K and the galactic background about 8K. If the mainbeam efficiency is 55 percent, the satellite antenna noise N_a would be

$$N_a = 0.55(260) + 0.25(94) + 0.2(8) \quad (1)$$

$$= 168 \text{ K}$$

The mobile antenna temperature might be 20% ground temperature and 80% sky temperature. At 850 MHz, galactic noise and emission noise from the atmosphere are both about 8K and additive. Hence, at the mobile, the antenna temperature N_a is given by

$$T_a = 0.2(260) + 0.8(8) + 0.8(8) \quad (16)$$

$$= 64.8 \text{ K}$$

Man-made noise may also add a component at the mobile as will solar noise but will be neglected here.

The system noise temperature T_s of the receiving system is given by

$$T_s = T_a + T_r$$

$$= 180 \text{ K} + 65 \text{ K}$$

$$= 245 \text{ K}$$

when $T_r = 180 \text{ K}$ is the assumed receiving system noise temperature (excluding T_a) referred to the antenna terminal.

3. Experiment Description

The starting point for the simulated land mobile satellite experiment was the National Scientific Balloon Facility in Palestine, Texas. This facility, sponsored initially by the NSF and associated with NCAR, was transferred to NASA in 1982. From Palestine, stratospheric balloons, reaching altitudes of 90,000 to 140,000 feet (27 to 43 km), are launched routinely throughout the year and especially around the few weeks in Spring and Fall when the winds in the upper atmosphere change direction and consequently slow down enough to allow for flights lasting tens of hours over land, within the boundaries of the U.S.A., and within the range of telemetry. The two communication experiments carried out in October, 1983 and January, 1984 had low weight requirements and therefore were attached ("piggy-backed") to other experiments. Since they were flown after the fall turn-around, the balloons drifted towards the east.

The major hardware components of the experiment were the transmitter borne by the balloon and the receiver and data acquisition system carried in a passenger van.

A block diagram of the transmitter is shown in Fig. 6. A Karkar KR900 communications transmitter produced 4 watts of output power. In addition to operating in CW mode it could be narrow band (25 KHz bandwidth) FM modulated, a feature that proved its value as an aid in the operation of the experiment, because it was used for occasional communication between the balloon base and the van. Powered by lithium batteries, the transmitter could be activated through the balloon control telemetry and operated for up to 30 hours.

The circularly polarized transmitter antenna, a drooping crossed dipole built from JPL specifications, was mounted on a ground plane of 2.6 wavelengths diameter. Impedance matching resulted in a return loss of better than 25 dB. The antenna assembly was mounted off the balloon axis and below the gondola in order to prevent any blockage (Fig. 7). The antenna pattern was not measured for this experiment, but assumed to be approximated by its theoretical pattern.

The receiving antenna was identical to the transmitting antenna, except that it was mounted on a 4 by 8 foot ground plane which was supported above the roof of the van (Fig. 8). The noise temperature of the receiver was 180K, resulting in a signal to noise ratio of about 30 dB at a range of 130 km and 20 degrees of elevation. The 869.525 MHz signal was filtered, amplified by a low noise FET amplifier, and converted to 29.525 MHz. The back-end consisted of a modified ICOM IC-R70 amateur radio communications receiver.

The receiver was operated simultaneously in the FM mode for the voice reception as well as in the AM mode with a predetection bandwidth of 14 Hz for the measurement of the signal power. A dynamic range exceeding 80 dB could be achieved by switching the rf gain of the receiver. The instantaneous dynamic range (at constant gain) was better than 30 dB.

The data acquisition system consisted of an IBM-PC with a Data Translation DT2801 board. The control program ran under PC-DOS 2.0 and was written in Fortran, using the SuperSoft compiler. Inputs to the program were the output voltage of the receiver, the discriminator voltage, and the speed of the van. The major experimental requirements were to:

- Control the rf gain of the receiver so that the peak signal voltage fell into a suitable range of the A/D converter.
- Measure the frequency of the received signal and insure that the receiver was tuned properly.
- Sample the signal at intervals of 1/8 wavelengths.
- Store the data together with pertinent system information on the floppy disks.

The signal was sampled in bursts of 1 second duration; and after some calculations were performed and adjustments made to the receiver, the next burst of sampling occurred. The duty cycle of this was about 60 percent. Every 4 to 5 minutes the data were transferred from memory to floppy disk.

In order for the van to follow the balloon, information about the approximate position, speed, and direction of the balloon had to be available in the van during the flight. This was accomplished over a duplex circuit. Transmission from the van to the balloon was at about 150 MHz, using a portable radio. This signal was relayed over the 1.5 GHz telemetry system to the balloon base. In the other direction, the voice was transmitted from NSBF to the balloon at 150 MHz and relayed to the van over the 869.525 MHz link. The quality of this signal was usually excellent because of the large signal to noise ratio in the receiver.

The experiment has been carried twice. Following a sunset launch on 10 October 1983, data were collected for some 8 hours while the van travelled about 600 km from Palestine, Texas over secondary roads through East Texas pine forests to Monroe, Louisiana. Elevation angles were in the range from 10 to 30 degrees. The second flight, on 11 January 1984, provided 2 hours of data at elevation angles between 27 and 35 degrees, again through East Texas.

4. Results of the Measurements

Two timeplots of received power levels, selected because they represent the range of signal variations observed, have been combined in Fig. 9. One shows both the effects of reflection and of shadowing (blockage) by trees. The van was driving on a two-lane road through a pine forest, and the line of sight to the balloon, at an elevation of 28 degrees, was visually observed to occasionally graze the treetops. The normalized variance, defined by:

$$\text{var} = 10 \log \frac{\langle (v - \langle v \rangle)^2 \rangle}{\langle v \rangle^2}$$

where v is the signal voltage and $\langle \rangle$ denotes taking the mean, was -9.2 dB. At the speed of 55.2 miles per hour, the van travelled about 75 wavelengths in one second and thus about 600 samples were taken over this distance. If one assumes the van to be a probe sampling a standing wave field set up by interference between the direct wave and ground reflections, then the sampling rate was about twice the one required to resolve the fields. Field strength variations caused by shadowing are also assumed to be fully resolved. The other one-second record shown was taken while the van was crossing a long two-lane causeway with steel guard rails over the Toledo Bend Reservoir at the Texas/Louisiana border. The elevation angle to the balloon was about 20 degrees and there was no shadowing at all. The -35.3 dB variance indicates that there was no scattering problem either.

Frequency spectra of the amplitude variations of the received signal voltage have been calculated and an estimate of their statistics has been made. The typical spectrum shown by the central line in Fig. 10 is based on about 100 seconds of data collected over about 5 minutes at a speed near 55 miles per hour. It was derived by applying a Fast Fourier Transform to the first 512 samples of each 1-second data record, resulting in a frequency resolution of about 1.2 Hz and a maximum frequency of about 300 Hz. After windowing the spectral components the power was calculated and smoothed with a seven element sliding triangular window. Finally, in

order to get a nearly equal spacing of points when plotting on a logarithmic frequency scale, a constant Q filter was applied to the data. The information about the severity of the fluctuations was removed by normalizing the area under the curve after summing the individual spectra. The result shown is typical in that it shows a slope of about 10 dB per decade in the region between about 10 and 100 Hz, followed by a steep decline in power at about 125 Hz. At a speed of 25 m/s (meters per second) through a standing wave field produced by the interference of 369 MHz wave-components traveling in opposite directions, the maximum expected amplitude modulation frequency would be $v/(wavelength/2)$ or 150 Hz.

The upper and lower curve in Fig. 10 give the power levels below which 5 and 95 percent of the individually normalized 1-second spectra were found to lie. The band between these contains 90 percent of all the measured spectra, but it should be noted that due to the normalization the bounds themselves are not spectra, since those which start out at a higher level, for instance, must fall off sooner than those starting lower. A fading channel in which a direct wave combines with randomly reflected waves can be described by the Rician probability distribution, which can be expressed in terms of the received power as

$$P\{s\} = (1+K) * \exp[-s(1+K)-K] * I_0(2\sqrt{s(1+K)K})$$

where K is the ratio of the specular to the random power received. The resulting probability distribution functions for K from 0 to 25 have been plotted in Fig. 11 for comparison with distribution functions measured at various elevation angles. The most obvious difference between the measured and predicted distributions is the sharper turn towards lower power at probabilities above about 90 or 95 percent. The data show improving power levels with increasing elevation angle with the exception of the 20 to 25 degree data, which were subjected to the most shadowing. Table I summarizes these results.

Table I
Power Distribution vs. Elevation

Elevation (degrees)	I	Signal Level in dB Rel. To FSL Exceeded at Probability of		
		50%	90%	95%
15 <= elev < 20	I			
	I	-1.0	-7.0	-10.8
	I			
20 <= elev < 25	I	-1.5	-9.8	-13.0
	I			
25 <= elev < 30	I	-0.5	-1.2	-2.0
	I			
30 <= elev < 35	I	-0.5	-1.2	-2.0

In order to separate the short- and long-term characteristics of the signal, the power levels exceeded for 50, 70, 90, and 95 percent of the time in each of the 1-second data records have been determined and their distributions (all elevation angles included) have been plotted in Fig. 12. The power level distribution of the same set of data has been included for comparison. The figure demonstrates that when 95 percent link availability is required, for instance, the overall statistics indicate an 8 dB margin. If one is not allowed to average over a long time (distance) but demands the 95 percent availability every second, however, then a 20 dB margin would be necessary. Considering that most of the data collected so far have been obtained at the low end of the applicable elevation angle range and in densely forested areas, these rather severe results should not be taken to rule out land mobile satellite communication. In the 30 to 35 degree elevation range, the measurements predict much more reasonable 95 percent margin requirements of 2 dB and 4 dB respectively. One way to overcome the extreme margin requirements would be by coding schemes which can cope with lower instantaneous link availability.

The fade duration is defined as the number of wavelengths the signal is below a threshold. It has been found that most of the 10 dB fades are shorter than one wavelength (or 14 ms for a car driving 55 mph) at elevation angles between 10 and 35 degrees, and 90 percent are shorter than two wavelengths at elevations under 30 degrees, and shorter than 5 wavelengths in the 30 to 35 degree range.

The level crossing rate is defined by how many times per wavelength an increasing signal crosses the threshold. Again, for the 10 dB fade level, rates of .5 to .7 crossings per wavelength are average and 90 percent of the crossing rates are below 2 per wavelength.

5. Comparison With Other Work

There are two other studies which lend themselves to direct comparison with this one. These are the Motorola measurements of ATS-6 by Hess (1980) and the Canadian work published by Butterworth and Matt (1983) and by Huck and co-workers (1983). A comparison with Hess published urban data in Figure 12 gives a good indication of the greater loss encountered under urban conditions. Hess did create a series of models, taking cognizance of most of the variables we recognize today. For comparison purposes, his 90% spatial 90% suburban rural value for required margin is plotted in Figure 12. We have analyzed our results, among other ways, along the lines that Hess has used: i.e., called short-term variation temporal (within one second), and then the variation of one-second levels (e.g., median or 90% of data) the spatial variation. In fact, of course, both variations are primarily spatial as can be seen by comparison with records when the vehicle is stationary.

Comparison of our data with that published by our Canadian Colleagues is shown in Figure 13. Their data is the result of helicopter-borne beacons over a stretch of land near Ottawa. Whereas the balloon flights give closer simulation to satellites, the balloon trajectories are not closely predictable so one works under less controlled conditions. For example, our data in the 20°-25° range is strongly influenced by a wide pine forest which happened to be present while the balloon was being observed at those altitudes. However, the general agreement is surprisingly good.

6. Conclusion

The program outlined here represents an attempt to satisfy two requirements. One is to test the theory of wave propagation as it is applied to land mobile satellite communication systems, and the other is to provide designers of these systems with design equations which preferably are based on sound theoretical considerations and whose parameters have been established by measurements. Ideally a prediction of the reliability of these communication links can be made if the area of operation in the U.S., receiver parameters such as bandwidth, coding scheme, or antenna pattern, and the position and pertinent characteristics of the satellite are known. For that purpose it will be necessary to acquire propagation data over the whole spectrum of topologies, such as flat, rolling, or mountainous, and for vegetation cover such as desert, shrub, crop, or forest. Such measurements are now planned together with systematic measurements of foliage attenuation. The enlarged data base will make it possible to better quantify the statistical characteristics of land mobile satellite communication.

FIGURE CAPTIONS

1. Artist's conception of land mobile satellite system with geostationary satellite. The direct ray r_1 and the specularly reflected wave r_2 combine to form the coherent component which is then combined with the Rayleigh-distributed diffuse component r_3 in a Nakagami-Rice distribution.
2. Observed Faraday rotation for transmissions from a midlatitude station to a geostationary satellite. Derived from Table VI, CCIR Report 263-5 (1977-78 and 1979-80 measurements from Tokyo of satellite ETS-II).
3. Plane earth ground reflection coefficients for sea water, fresh water and three different sets of ground constants for a frequency of 1 GHz.
4. Terrain roughness factor as determined by two different formulas.
5. Construction illustrating the maximum Doppler fade rate (signal scattered from behind the vehicle when it moves towards the satellite with velocity v).
6. Block diagram of the balloon-borne transmitter.
7. Photograph of the transmitting antenna assembly mounted off the balloon axis and below the gondola to prevent blockage.
8. Photograph of the drooping dipole receiving antenna mounted under a radome on a 4 by 8 foot ground plane above the roof of the van.
9. Two one second time plots of received signal level. Shown in A is a sample taken along a causeway where no signal blockage was encountered; while B was taken in a pine forest where signal blockage did occur.
10. Frequency spectra (normalized and smoothed) of a 100 second sample of data when the van was moving at 55 miles per hour.
11. Values of K , the ratio of specular to random power, for the Rice-Nakagami distribution compared with data taken at different elevation angles.
12. Plot of signal level distribution for 50%, 70%, 90%, and 95% of the time inside each 1 second period with power level distribution also shown. Also shown for comparison is Hess' (1980) results for urban Denver (90% spatial, 90% temporal).
13. Comparison of data from Vogel and Torrence (1984) with helicopter data obtained by Butterworth et al. (1983). Inconsistency between the 15°-20° curve and 20°-25° curve is due to excess foliage attenuation in the latter data sample.

REFERENCES

Anderson, R. E., R. L. Frey, J. R. Lewis and R. T. Milton, "Satellite-Aided Mobile Communications: Experiments, Applications and Prospects," IEEE Transactions on Vehicular Technology, VT-30, 2, 54-61, May, 1981.

Butterworth, J. S. and E. E. Matt, "The Characterization of Propagation Effects for Land Mobile Satellite Services," IEE Conference Publication No. 222: Satellite Systems for Mobile Communications and Navigation, 51-94, 1983.

Beckmann, P. and A. Spizzichino, "The Scattering of Electromagnetic Waves from Rough Surfaces," Pergamon Press, 1963.

CCIR XVth Plenary Assembly, Geneva, 1982, Volume V, "Propagation in Ionized Media:" International Telecommunication Union, Geneva, Switzerland:

-Report 236-5 "Influence of Terrain Irregularities and Vegetation on Tropospheric Propagation" (provisionally updated by Document 5/209 of the Study Group V Interim Meeting, November 1983).

-Report 720-1 "Radio Emission from Natural Sources above 50 MHz."

-Report 884 "Propagation Data for Maritime and Land Mobile Satellite Systems at Frequencies above 100 MHz." (Provisionally updated by Rep. AF/5 of Doc. 5/209).

CCIR XVth Plenary Assembly, Volume VI "Propagation in Ionized Media:"

-Report 263-5 "Ionospheric Effects upon Earth-space propagation."

Flock, W. L., "Propagation Effects on Satellite Systems at Frequencies below 10 GHz: A Handbook for Satellite System Design," NASA Reference Publication 1108. December, 1983. For sale by the National Technical Information Service, Springfield, VA 22161.

Hess, G. C., "Land Mobile Satellite path Loss Measurements," Third year ATS-6 Experiment Final Report; September 6, 1978; R. F. Systems Lab., Motorola Inc., Schaumburg, Illinois.

Hess, G. C., "Land-Mobile Satellite Excess Path Loss Measurements," IEEE Transactions on Vehicular Technology, Vol. VT-29, No. 3, 290-297, 1980.

Horstein, M., "Requirements for a Mobile Communications Satellite System," Vols. I & II, TRW, Inc. Final Report, NASA/Lewis Contract NAS3-23257, April 11, 1983.

Huck, R. W., J. S. Butterworth and E. E. Matt, "Propagation Measurements for Land Mobile Satellite Services," IEEE 33rd Vehicular Technology Conference Rec -J, 265-268, 1983.

Kiesling, J. D. and R. Anderson, et. al., "Mobile Radio Alternatives System Study," General Electric Final Report, NASA/Lewis Contract NAS3-23244, June 1983.

Miller, A. R. , R. M. Brown, and E. Vegh, "New Derivation for the Rough-Surface Reflection Coefficient for the Distribution of Sea Wave Elevations," IEE Proceedings, Vol. 131, Pt. H, No. 2, April, 1984.

Naderi, F., Ed., "Land Mobile Satellite Service (LMSS): A Conceptual System Design and Identification of the Critical Technologies," Jet Propulsion Laboratory Publication 82-19, Feb. 15, 1982.

Naderi, F., G. H. Knouse and W. J. Weber, "NASA's Mobile Satellite Communications Program; Ground and Space Segment Technologies," presented at the International Astronautics Federation Congress, Laussane, Switzerland, Oct. 1984.

Smith, E. K., J. F. Cavanagh and W. L. Flock, "Propagation Effects for Land Mobile Satellite Systems" National Radio Science Meeting, sponsored by USNC/URSI and IEEE, Commission F, 5-7 January, 1983.

Vogel, W. F. and G. W. Torrence, "Measurement Results from a Balloon Experiment Simulating Land Mobile Satellite Transmissions," MSAT-X Report 101, available through E. K. Smith, MS 161-228, Caltech Jet Propulsion Laboratory, Pasadena, CA 91109, 1984.

Weissburger, M. A. "An Initial Critical Summary of Models for Predicting the Attenuation of Radio Waves by Foliage," ECAC-TR-81-101, Electromagnetic Compatibility Analysis Center, Annapolis, MD., Aug. 1981.

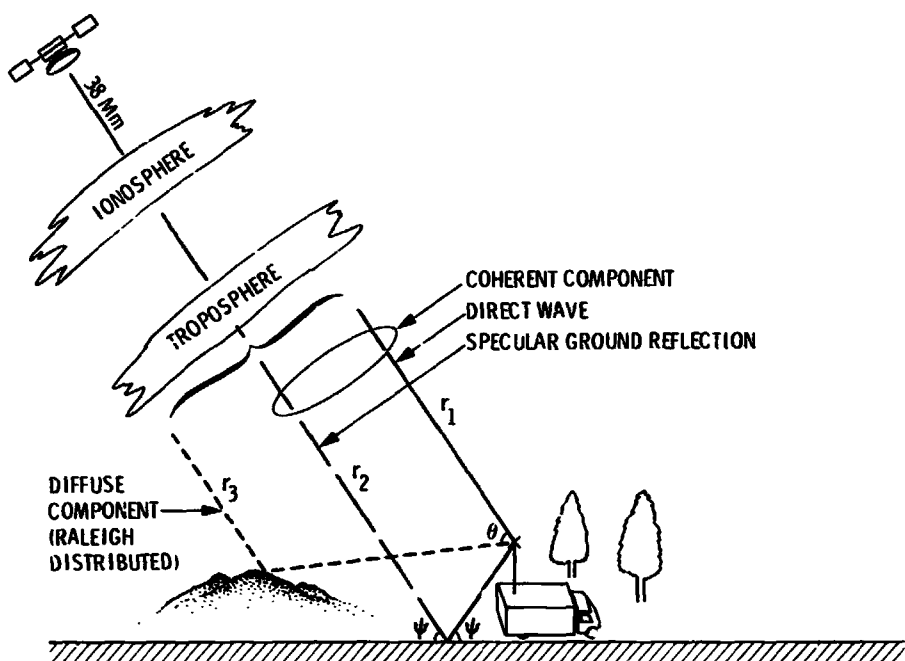


Figure 1

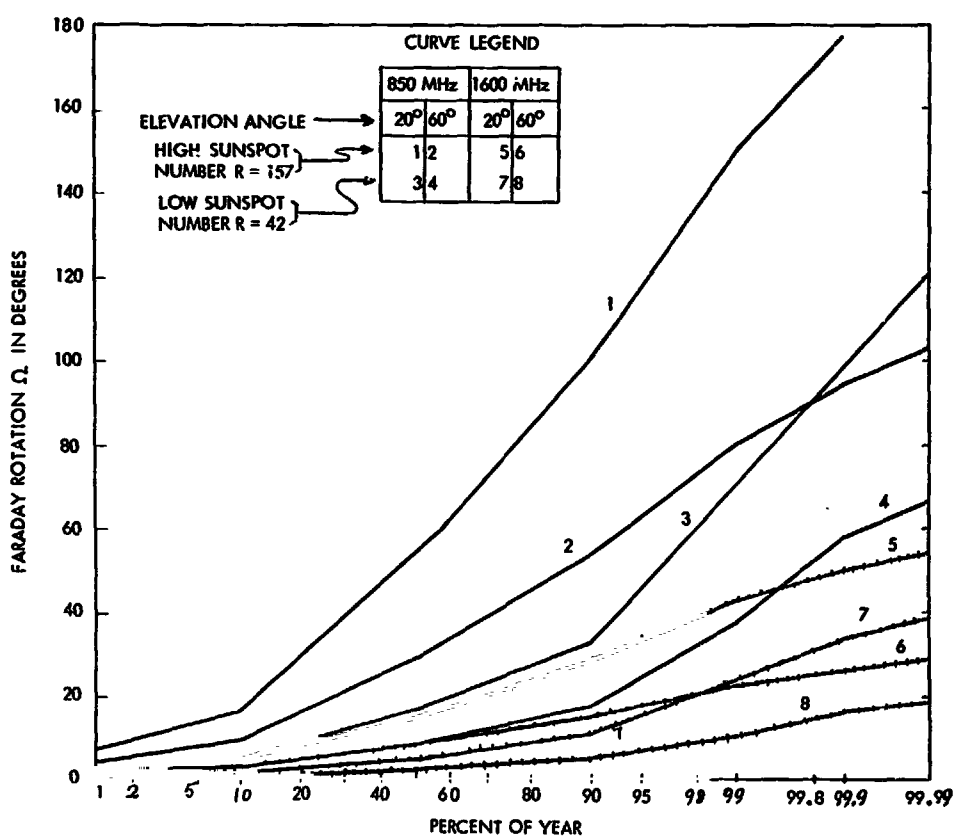


Figure 2

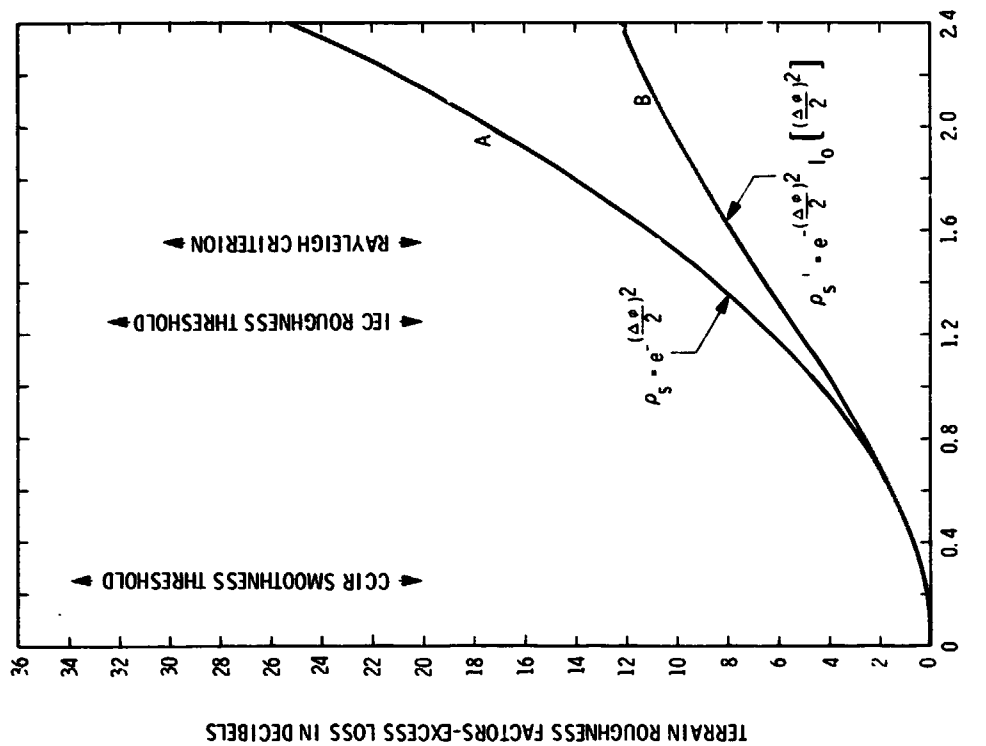


Figure 4

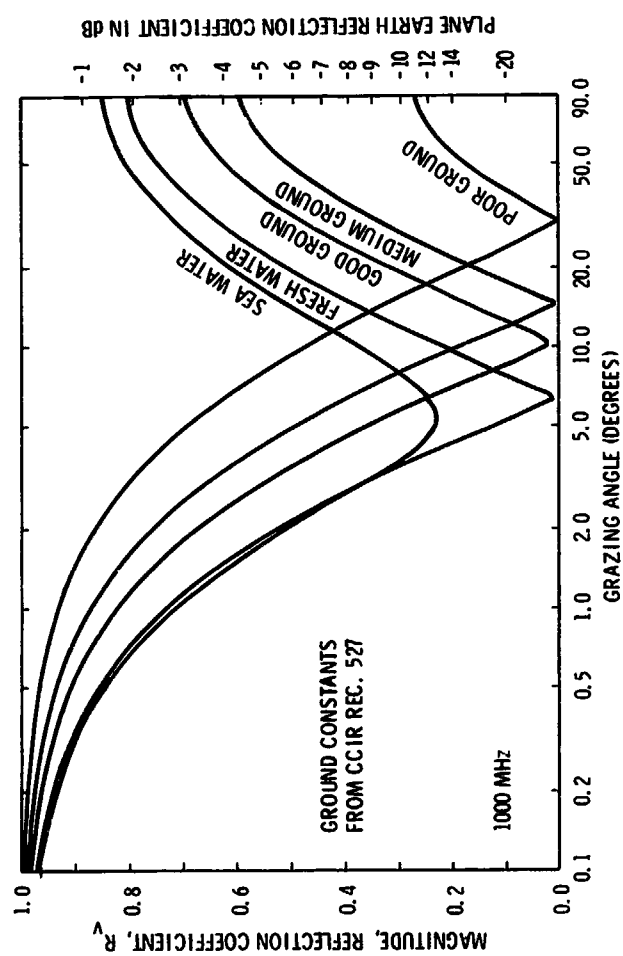


Figure 3

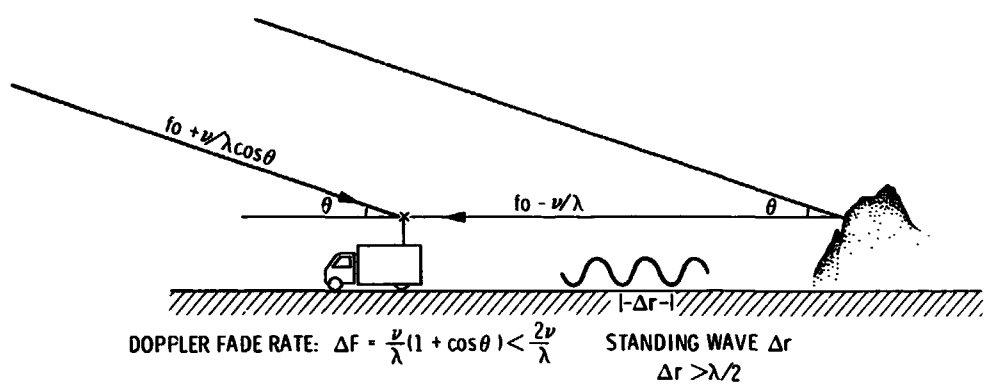


Figure 5

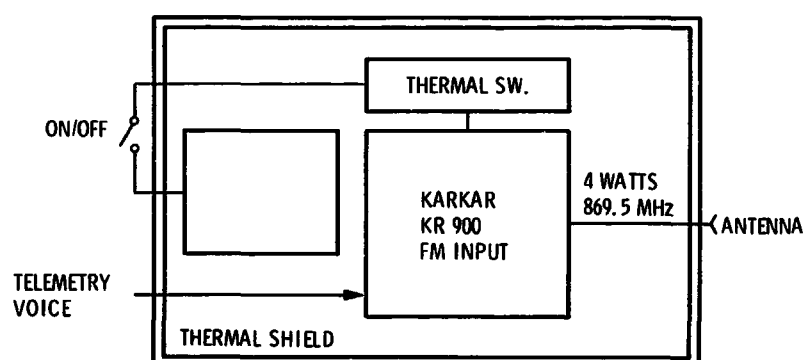


Figure 6

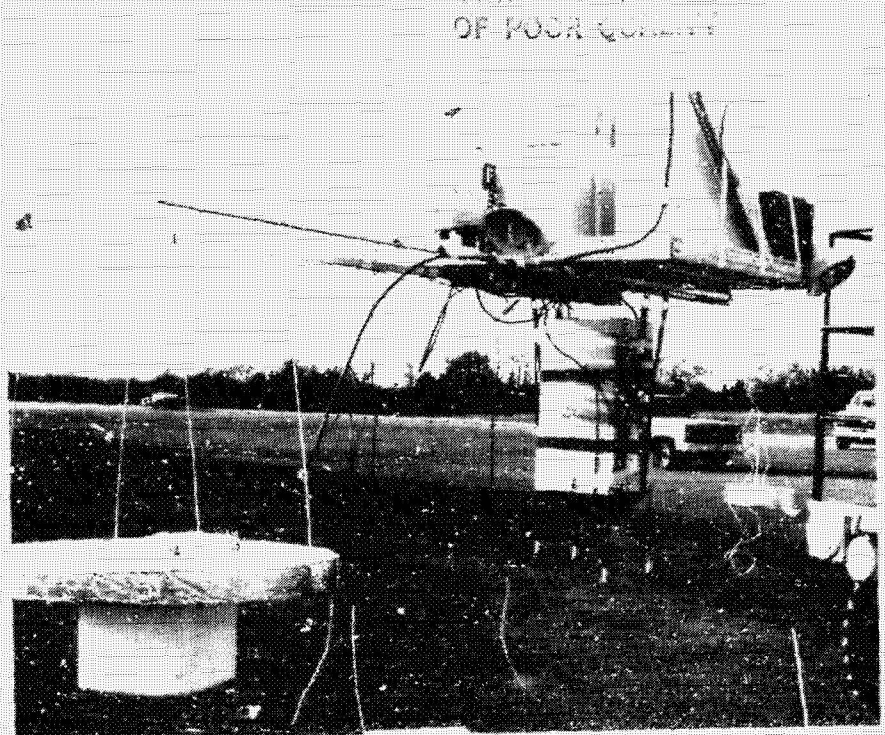


Figure 7



Figure 8

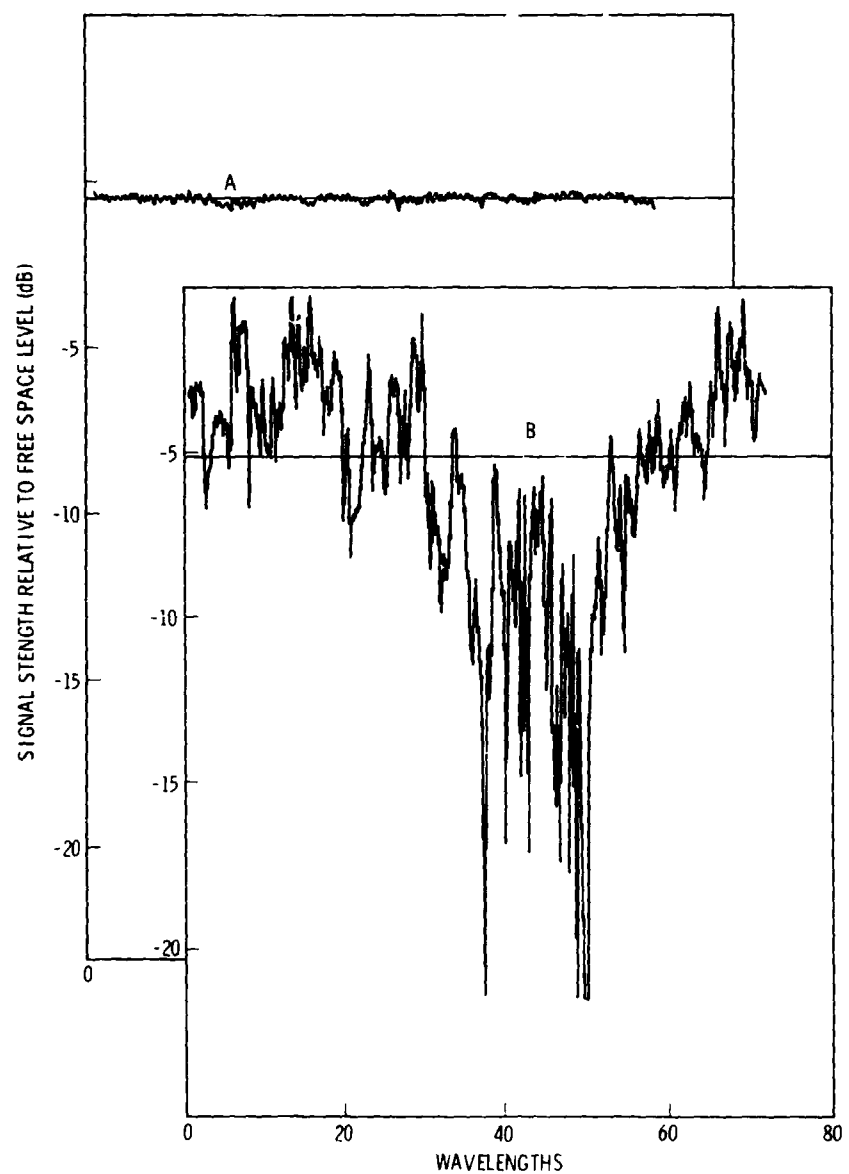


Figure 9

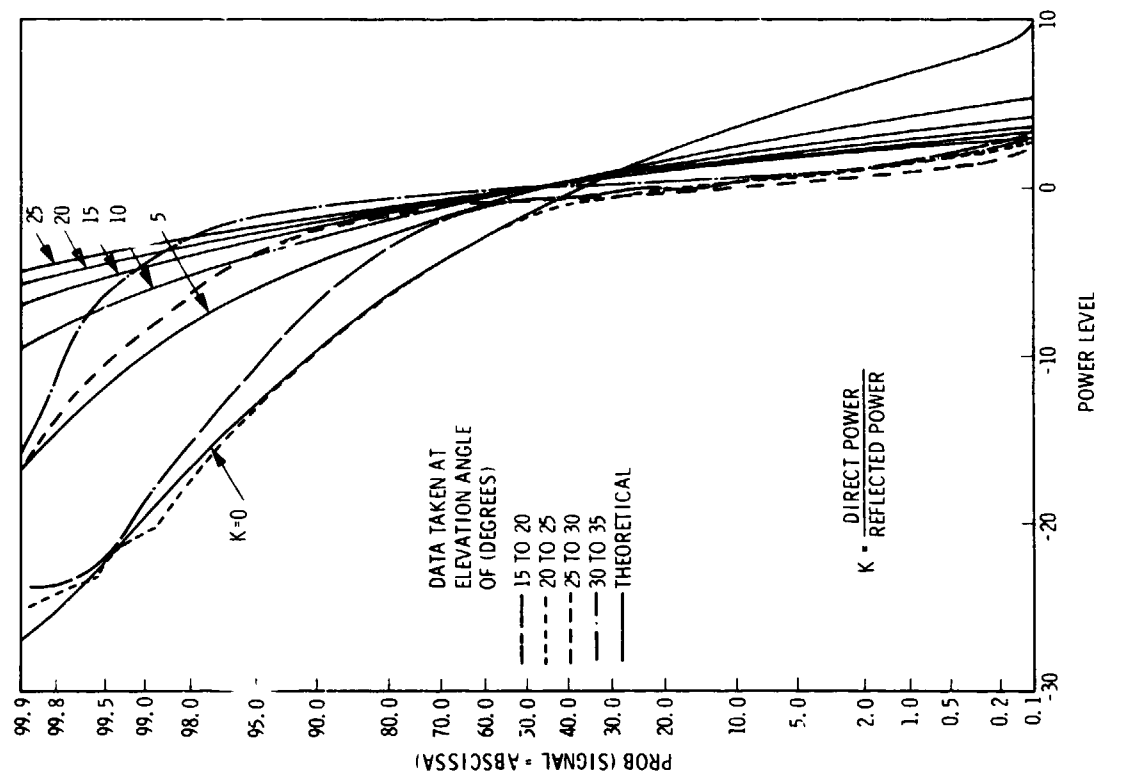


Figure 11

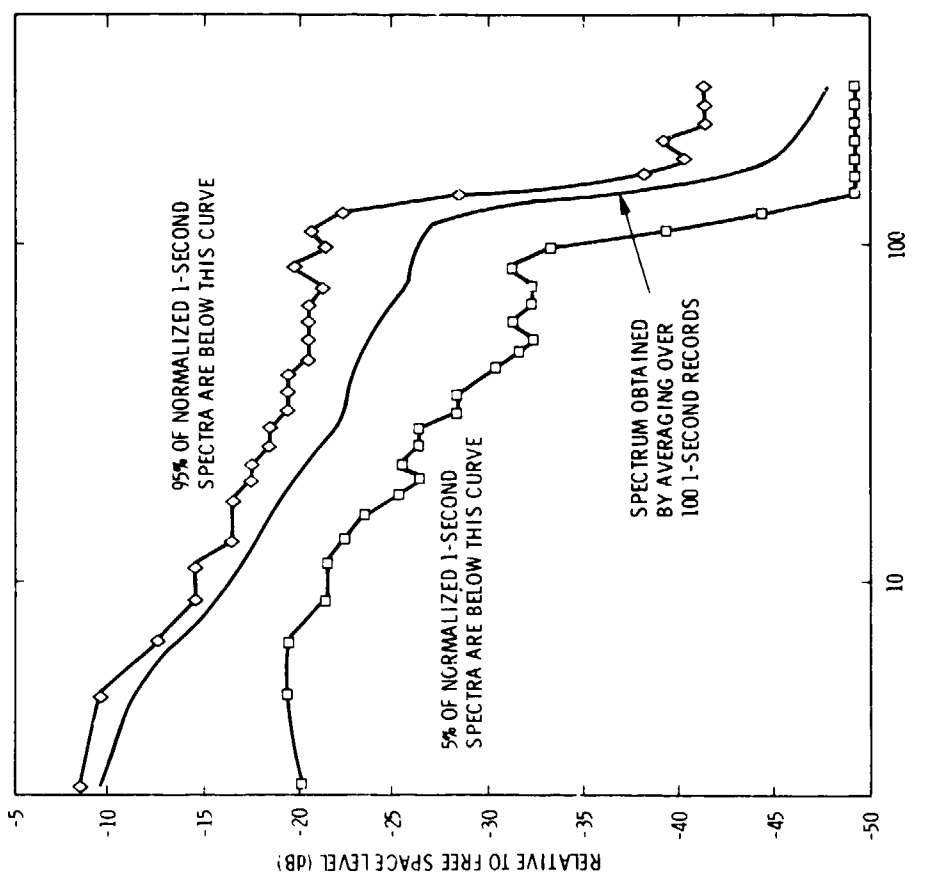


Figure 10

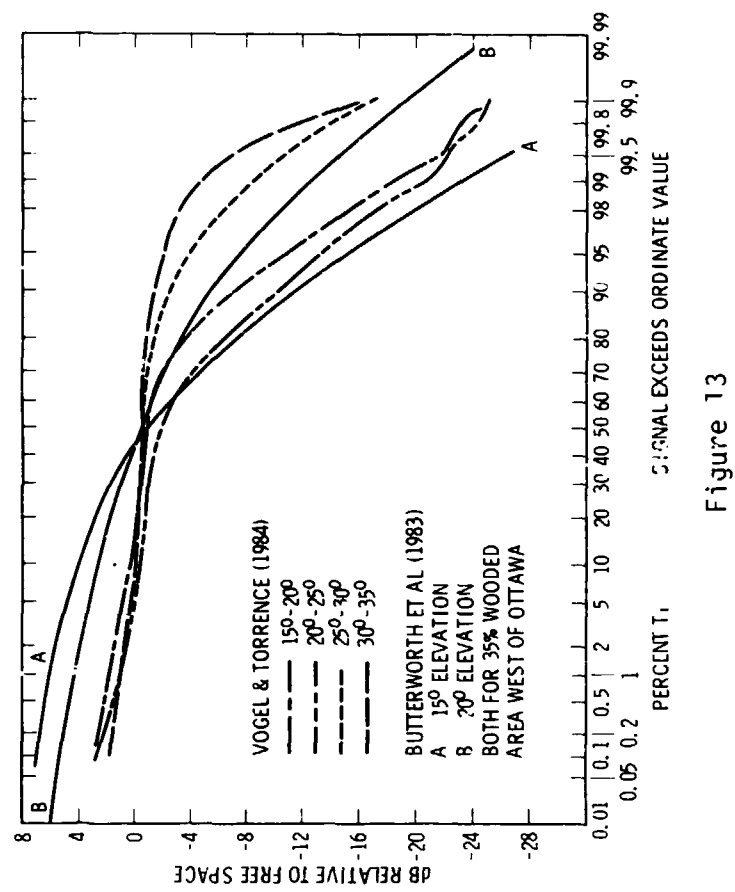


Figure 13

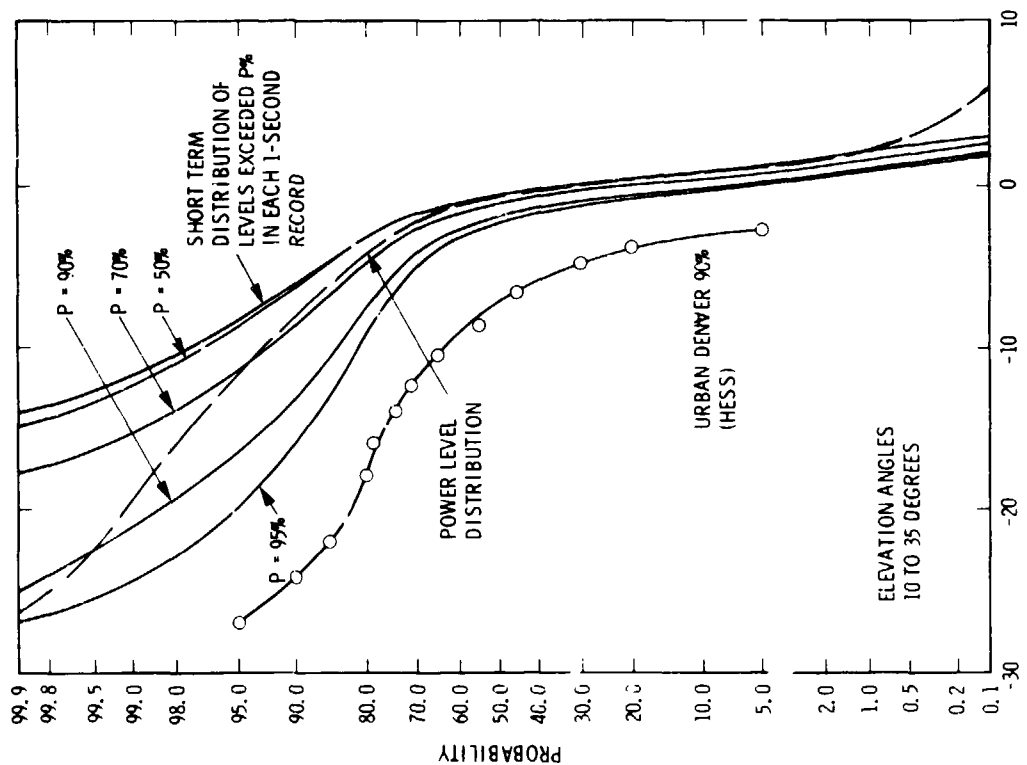


Figure 12